



**HAL**  
open science

# Dissipation Effect on Local and Global Fluid-Elastic Instabilities

Olivier Doaré

► **To cite this version:**

Olivier Doaré. Dissipation Effect on Local and Global Fluid-Elastic Instabilities. Oleg N. Kirillov, Dmitry E. Pelinovsky. *Nonlinear Physical Systems: Spectral Analysis, Stability and Bifurcations*, John Wiley & Sons, 2014, 10.1002/9781118577608.ch4 . hal-01140892

**HAL Id: hal-01140892**

**<https://ensta-paris.hal.science/hal-01140892>**

Submitted on 9 Apr 2015

**HAL** is a multi-disciplinary open access archive for the deposit and dissemination of scientific research documents, whether they are published or not. The documents may come from teaching and research institutions in France or abroad, or from public or private research centers.

L'archive ouverte pluridisciplinaire **HAL**, est destinée au dépôt et à la diffusion de documents scientifiques de niveau recherche, publiés ou non, émanant des établissements d'enseignement et de recherche français ou étrangers, des laboratoires publics ou privés.

# Dissipation effect on local and global fluid-elastic instabilities

Olivier Doaré

Chapter published in:

*Nonlinear Physical Systems: Spectral Analysis, Stability and Bifurcations*, Chapter 4, 67-84, Kirillov & Pelinovsky editors, John Wiley & Sons publisher.

## 1 Introduction

In many physical systems, damping has been observed to have a stabilizing or destabilizing effect. The latter effect is counter-intuitive, as a stable system without damping should indeed remain stable if dissipative forces are added. Various discrete mechanical systems display this unusual feature. The most famous is probably that studied by Ziegler in 1952 [40]. It consists of a double-pendulum subjected to a follower force, which can be practically achieved by dry friction [6, 5]. It was found by Ziegler that the critical value of the load at which the straight equilibrium position becomes unstable decreases and changes in a discontinuous manner when an infinitesimal amount of viscous damping is added in the model. Many gyroscopic systems presents this feature [32, 20], as well as aeroelastic systems [23] and the experimental evidence of a destabilizing effect of a viscous fluid has been obtained in the the context of rotor dynamics [2, 17]. In the case of a general dynamical system, Bottema [8] has described the required conditions for the damping to induce instability. After Kirillov & Verhulst [20], the discontinuous behavior of the critical value of the parameter for instability is linked to the existence of singularities of maps between manifolds of dimension  $n$  to spaces of dimension  $2n - 1$ , as studied by Whitney [39] in a purely mathematical context, independently of the effect of dissipation on mechanical systems.

Destabilizing effect of damping in continuous, but finite systems, has also been evidenced. The cantilevered beam subjected to a follower force has been studied by Sugiyama & Langthjem [34] in terms of energy transfers at the free end. In the case of a fluid-conveying pipe, the stabilizing or destabilizing nature of damping has been shown to depend on the fluid-solid mass ratio [27]. Similar conclusions have been drawn for the fluttering flag [18].

In infinite systems described by wave equations, the effect of damping on stable waves has also been the aim of a large number of papers. In the problem

consisting of a flow over a compliant panel, Landahl [22] showed that viscosity was able to destabilize some neutral waves. The same phenomenon was observed in the fluid-conveying pipe problem [31]. The first scientific community faced to such destabilizing phenomena was that of plasma physics, where the concept of wave of negative energy was introduced [38, 9, 4]. This concept has been a considerable addition to the discussion at stability of these media and has been introduced in the research field of mechanics by Cairns [10], who showed that the classical expression of the wave energy introduced in plasma physics represents here the work done on the system to generate the wave from  $t = -\infty$  to  $t = 0$ .

The objective of this chapter is to present a joint local/global stability analysis of a model problem of fluid-elastic instabilities: the fluid-conveying pipe. As emphasized in a recent review by Païdoussis [30], the fluid-conveying pipe may be seen as a model problem for many physical systems where a slender structure is coupled to an axial flow, and has applications in many fields, such as paper and nuclear industries, aeronautics, musical acoustics or biomechanics. The fluid-conveying pipe share many similarities with all the systems mentioned above: once a critical value of a parameter is reached (here the flow velocity) the finite length system exhibits an instability and damping can in some cases lower the critical velocity value. In the infinite length system, unstable waves (temporally or spatially amplified) may be identified as well as neutral waves that become unstable waves when a small amount of damping is added. However, in none of the above-cited works, a joint local and global analysis is performed to determine which role the negative energy waves play in the global instability.

This chapter is organised as follows: In the next section, the local and global analyses are briefly described. Next, the linear equations governing the dynamics of a fluid-conveying pipe are presented. Local and global stability analyses of this system are then performed. An application to energy harvesting is finally proposed and a conclusion closes the chapter.

## 2 Local and global stability analyses

In this section, the local and global instability analyses of a general one-dimensional mechanical system are presented.

### 2.1 Local analysis

Consider an infinite length one-dimensional medium governed by a wave equation of the form,

$$\frac{\partial^2}{\partial t^2} \mathcal{M} [y(x, t)] + \frac{\partial}{\partial t} \mathcal{C} [y(x, t)] + \mathcal{K} [y(x, t)] = 0 \quad \text{on } \Omega = [-\infty, +\infty], \quad (1)$$

where  $\mathcal{M}$ ,  $\mathcal{C}$  and  $\mathcal{K}$  are mass, damping and rigidity operators respectively. Introducing in this equation a disturbance of the form of a plane harmonic wave

$y = y_0 e^{i(kx - \omega t)}$  leads to a dispersion relation that links frequency to wavenumber,

$$D(k, \omega) = 0. \quad (2)$$

The medium is stable if, for any sinusoidal wave of infinite extent in the  $x$ -direction and associated to a real wavenumber  $k$ , the corresponding frequencies given by equation (2) are such that the displacement remains finite in time. The *local* instability criterion is then,

$$\text{Instability if } \exists k \in \mathbb{R} \setminus \text{Im}[\omega(k)] > 0. \quad (3)$$

This approach is said to be *temporal*, since it consists in examining the *temporal* evolution of waves in time.

## 2.2 Global analysis

The global analysis considers the same local wave equation (1) in a finite domain  $\Omega = [0, l]$ , associated with a set of boundary conditions, denoted as  $\mathcal{B}_i(y) = 0$   $i = 1..N$ , where  $N$  is the maximal order of the spatial derivatives in operators  $\mathcal{K}$  and  $\mathcal{M}$ . Considering ansatz solutions of the form  $y = \phi(x)e^{-i\omega t}$ , one obtains a Sturm-Liouville problem which solutions are an infinite set of eigenfunctions  $\phi_n(x)$  and eigenfrequencies  $\omega_n$ . In this case, the instability condition reads,

$$\text{Instability if } \exists \omega_n \setminus \text{Im}[\omega_n] > 0. \quad (4)$$

Numerical methods are generally used to solve this kind of problems. In the following, a Galerkin method is used to compute approximate solutions. The solution  $y(x, t)$  is decomposed on a truncated function basis that satisfies the boundary conditions,

$$y(x, t) = \sum_{n=1}^N \psi_n(x)q(t). \quad (5)$$

After defining a scalar product,

$$\langle f, g \rangle = \int_{\Omega} f g dx, \quad (6)$$

the approximated form of  $y$  defined in equation (5) is introduced in (1), which is then projected on a mode  $\psi_m(x)$ . One finally obtains a discrete set of coupled oscillator equations,

$$M\ddot{\vec{q}} + C\dot{\vec{q}} + K\vec{q} = 0. \quad (7)$$

The coefficients of the matrices  $M$ ,  $C$ , and  $K$  result from the projection of the inertia, damping and rigidity forces of equation (1). Finally, looking for harmonic solutions in the form of  $\vec{q} = \vec{q}_0 e^{-i\omega t}$  leads to a second order eigenvalue problem for the eigenfrequency. The criterion for global instability is then given by (4), and the corresponding eigenvector gives the eigenmode in the form of a combination of functions  $\psi_j(x)$ .

### 3 The fluid conveying pipe: a model problem

The simplest equation describing the linear dynamics of this system consists in an Euler-Bernoulli equation for a beam of mass per unit length  $m$ , flexural rigidity  $EI$ , in which an internal fluid of mass per unit length  $M$  and of negligible viscosity is flowing at the constant velocity  $U$ . The dimensional wave equation governing the vertical displacement  $Y(X, T)$  reads [29],

$$EI \frac{\partial^4 Y}{\partial X^4} + m \frac{\partial^2 Y}{\partial T^2} + M \frac{\partial^2 Y}{\partial T^2} + MU^2 \frac{\partial^2 Y}{\partial X^2} + 2MU \frac{\partial^2 Y}{\partial X \partial T} = 0 \quad (8)$$

The first two terms in this equation are the flexural rigidity and inertia terms of the linearized Euler-Bernoulli equation. The third term is an inertia term that from the presence of the fluid inside the pipe. The fourth term may be understood as a centrifugal term that arises as soon as the beam experiences a local curvature. Finally the fifth term is generally referred to as a Coriolis force and may be interpreted by considering a portion of the pipe moving at a constant velocity. Due to the presence of a moving mass inside, a force is exerted on this portion of the pipe.

When damping is to be considered, one may add one or both of these two additional forces to the wave equation,

$$\mathcal{D}_f(Y) = C \frac{\partial Y}{\partial T}, \quad \mathcal{D}_s(Y) = E^* I \frac{\partial^5 Y}{\partial X^4 \partial T}. \quad (9)$$

The first case is referred to as viscous damping and is generally a consequence of the presence of a viscous fluid around the pipe, while the second is called structural damping and is the consequence of a viscoelastic behavior of the material that constitutes the pipe.

After introducing the characteristic length  $\eta = \left(\frac{EI}{MU^2}\right)^{1/2}$  and time  $\tau = \left(\frac{(m+M)\eta^4}{EI}\right)^{1/2}$  and rescaling all dimensional quantities using these two parameters, the wave equation takes a form that depends on only one independent parameter  $\beta$ ,

$$\frac{\partial^2 y}{\partial t^2} + \frac{\partial^4 y}{\partial x^4} + \frac{\partial^2 y}{\partial x^2} + 2\sqrt{\beta} \frac{\partial^2 y}{\partial x \partial t} = 0, \quad (10)$$

where  $\beta$  is the mass ratio,

$$\beta = \frac{M}{m+M} \in [0, 1]. \quad (11)$$

Note that the case  $\beta = 0$  is strictly equivalent of cantilevered beam with a follower force, referred to as the Beck's column [3]. In their dimensionless forms, the damping operators now write,

$$d_f(y) = c \frac{\partial y}{\partial t}, \quad d_s(y) = \alpha \frac{\partial^5 y}{\partial x^4 \partial t}. \quad (12)$$

When considering a finite length system, the non-dimensional length has to be introduced,

$$l = \frac{L}{\eta} = UL\sqrt{\frac{M}{EI}}, \quad (13)$$

and two boundary conditions have to be specified at each boundary. They read

$$y(x = x_0, t) = y'(x = x_0, t) = 0, \quad y''(x = x_0, t) = y'''(x = x_0, t) = 0, \quad (14)$$

for a clamped end and a free end respectively, where the primes  $(.)'$  denote derivation with respect to  $x$  and  $x_0$  takes the value 0 or  $l$ .

## 4 Effect of damping on the local and global stability of the fluid-conveying pipe

### 4.1 Local stability

The dispersion relation of the undamped fluid-conveying pipe reads,

$$D(k, \omega) = k^4 - \omega^2 + k^2 + 2\sqrt{\beta}k\omega = 0. \quad (15)$$

The frequency associated to a real wavenumber  $k$  then reads,

$$\omega_{\pm} = \sqrt{\beta}k \pm k\sqrt{\beta + k^2 - 1}. \quad (16)$$

For  $\beta \in [0, 1[$  and  $k \in [0, \sqrt{1 - \beta}]$ , frequencies  $\omega_{\pm}$  are complex conjugate and the positive imaginary part of one of them gives rise to a wave with an amplitude exponentially growing in time. For  $k > \sqrt{1 - \beta}$ ,  $\omega(k) \in \mathbb{R}$  and waves are said neutral. In conclusion the medium is locally unstable  $\forall \beta \in [0, 1[$ . Conversely for  $\beta \geq 1$ , the medium is neutrally stable. However, it has to be noted that  $\beta > 1$  has no physical meaning in the present context.

In various studies on the effect of damping on wave propagation, the key role of the wave energy has been evidenced. Although introduced in the context of shear layer waves between two non miscible fluids [10], the definition is generic and can be readily used in any mechanical system. Consider an harmonic wave with  $\omega$  and  $k \in \mathbb{R}$  and  $D(k, \omega) = 0$ . The wave energy is defined as the work done on the system to establish this neutral wave from  $t = -\infty$  to  $t = 0$ , and reads,

$$E = -\frac{\omega}{4} \frac{\partial D}{\partial \omega} y_0^2. \quad (17)$$

If  $E$  is negative, it means that energy has to be removed from the system to establish the wave. The latter is then referred to as a *negative energy wave* (NEW) [38].

Now consider that a small amount of viscous damping is added in the system, so that the dispersion relation takes the form,

$$D_1(k, \omega + \delta\omega) = D(k, \omega + \delta\omega) - ic(\omega + \delta\omega) = 0, \quad (18)$$

where  $\delta\omega \ll \omega$  is a small perturbation to the frequency introduced by the damping, which satisfies at order one,

$$\delta\omega \left. \frac{\partial D}{\partial \omega} \right|_{(k,\omega)} = ic\omega. \quad (19)$$

We readily deduce from this expression the perturbation on the growth rate  $\delta\sigma = \text{Im}(\delta\omega)$ ,

$$\delta\sigma = \frac{c\omega}{\partial D/\partial \omega}. \quad (20)$$

This quantity has the opposite sign of the wave energy  $E$ . A NEW is hence destabilized by viscous damping. The same calculation performed with viscoelastic damping gives:

$$\delta\sigma = \frac{\alpha k^4 \omega}{\partial D/\partial \omega}, \quad (21)$$

which leads us to the same conclusions.

In the fluid-conveying pipe case, the wave energy has for expression,

$$E_{\pm} = \frac{1}{2} k^2 \sqrt{k^2 + \beta - 1} \left( \sqrt{k^2 + \beta - 1} \pm \sqrt{\beta} \right), \quad (22)$$

and  $E_-$  has negative values in the range  $k \in ]\sqrt{1-\beta}, 1[$ . Hence, the range of temporally unstable waves becomes  $[0, 1[$  when damping is added, whereas it was  $k \in [0, \sqrt{1-\beta}]$  in the conservative case. Damping enlarged the range of unstable wavenumbers. Moreover, the system is now temporally unstable for any value of  $\beta$ , when it was for  $\beta \in [0, 1[$  in the conservative case.

On Fig. 1, the ranges of unstable wave in the damped and undamped cases are compared when the parameter  $\beta$ , quantifying the Coriolis force varies from 0 to 1. It can be concluded from this figure that Coriolis force stabilizes waves, which are in turn destabilized by a small amount of damping. The same kind of behavior was observed in discrete systems in 1879 by Thomson and Tait [36].

## 4.2 Global stability

Boundary conditions and finite length parameter  $l$  are now introduced. The dimensionless parameter  $l$  in equation (13) is proportional to both  $L$  and  $U$ , indicating that it can be seen as a dimensionless length or flow velocity. Although the limit  $l = 0$  has no meaning when it is sought as a length, it can be achieved by letting the flow velocity vanish. In the global approach, it is then more convenient to use  $L$  to rescale the lengths, so that the dimensionless wave equation becomes,

$$\frac{\partial^2 y}{\partial t^2} + \frac{\partial^4 y}{\partial x^4} + v^2 \frac{\partial^2 y}{\partial x^2} + 2\sqrt{\beta}v \frac{\partial^2 y}{\partial x \partial t} = 0, \quad (23)$$

where the length of the dimensionless problem being the unity and with,

$$v = l. \quad (24)$$

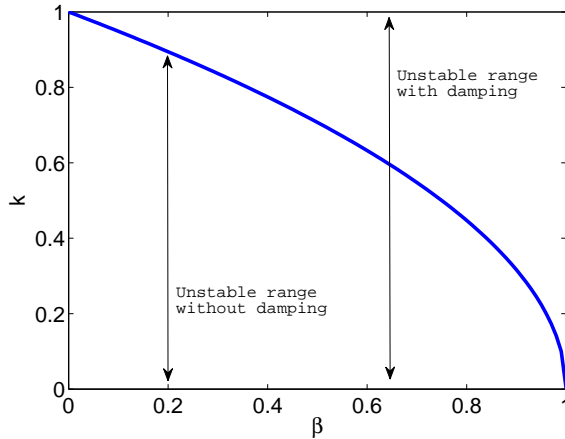


Figure 1: Range of unstable wavenumbers as function of  $\beta$ . This illustrates the fact that the range of wavenumbers  $\sqrt{1-\beta}$  is stabilized by the Coriolis force and this range is then destabilized when damping is added in the medium.

The Galerkin method presented in section 2.2 is used here to obtain the present results. The chosen test functions are the eigenmodes of the pipe without flow. The functions  $\psi_n(x)$  are hence the eigenfunctions of equation (23) with the same set of boundary conditions and  $v = 0$ . These eigenfunctions are basically the eigenmodes of a beam and are known and well documented analytic functions (see for instance the book by Blevins [7]). Equation (23) is then projected on each mode  $\psi_m$ , leading to  $N$  ordinary differential equations for the time variable, which read,

$$\ddot{\vec{q}} + 2\sqrt{\beta}v C \dot{\vec{q}} + (K_d + v^2 K_f)\vec{q} = 0. \quad (25)$$

The coefficients of the matrices  $C$ ,  $K_d$  and  $K_f$  result from the projection of the Coriolis, flexural rigidity and centrifugal operators respectively. Note that  $K_d$  is diagonal, as discussed above. The coefficients of these matrices can be found in the paper by Gregory & Païdoussis [16]. In the clamped-clamped case,  $C$  is skew-symmetric and  $K_f$  is symmetric. In the clamped-free case,  $C$  and  $K$  have both symmetric and skew-symmetric parts. This has consequences on the bifurcations properties of these two systems. The bifurcation types have been studied in such discrete systems. The role of matrix symmetries in the bifurcation is not in the scope of the present paper and can be found in other mathematical studies [19, 20].

#### 4.2.1 Evolution of eigenfrequencies and bifurcations

The evolution of the eigenfrequencies when  $v$  is increased from 0 is plotted on Fig. 2 in four typical cases: a pipe clamped at both ends, a clamped-free pipe



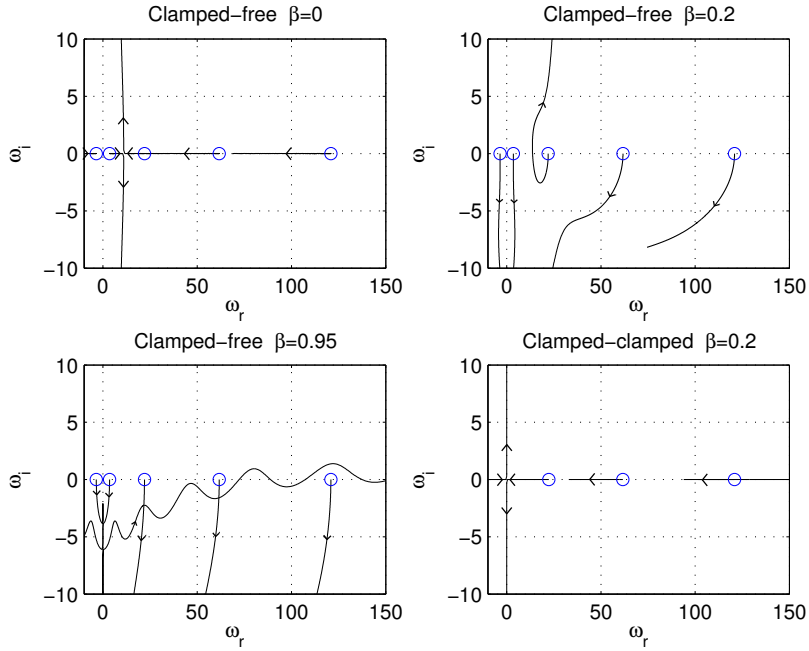


Figure 2: Evolution in the complex plane of the eigenfrequencies of the clamped-clamped and clamped-free pipe when the velocity parameter  $v$  is increased from zero, for different values of the mass ratio  $\beta$ .

at  $\beta = 0$ , and a clamped-free pipe at  $\beta = 0.2$  and  $\beta = 0.95$ . These graphs illustrate the typical behaviors of the eigenfrequencies when the flow velocity is increased. Different bifurcations are evidenced. In the case of a clamped-clamped pipe, instability always arises through a saddle-node bifurcation. The instability is called static instability, or buckling. In the case of a clamped-free pipe, the bifurcation depends on the value of the mass ratio  $\beta$ . If  $\beta = 0$ , the dissipation matrix vanishes in equation (25) and the instability occurs via a Hopf bifurcation after the merging of two eigenfrequencies on the real axis. In the fluid-elastic community, this instability is referred to as flutter instability, as it results in self-sustained oscillations of the structure once the amplitude of the solution has been saturated by the non-linear effects. When  $\beta \neq 0$ , the increase of the flow velocity has at first a stabilizing effect, due to a flow-induced damping through the matrix  $C$ : all the eigenfrequencies travel towards the negative imaginary part half plane. When further increasing the flow velocity, one eigenfrequency changes its trajectory and crosses the real axis, giving rise to a flutter instability.

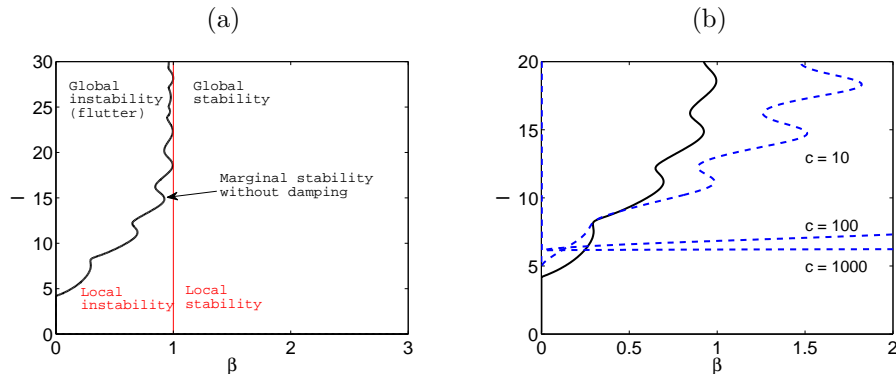


Figure 3: (a), marginal global stability curve of the pipe conveying fluid in the parameter plane  $(\beta, l)$  (thick black) compared with the local stability criterion; (b), marginal global stability curves for increasing viscous damping.

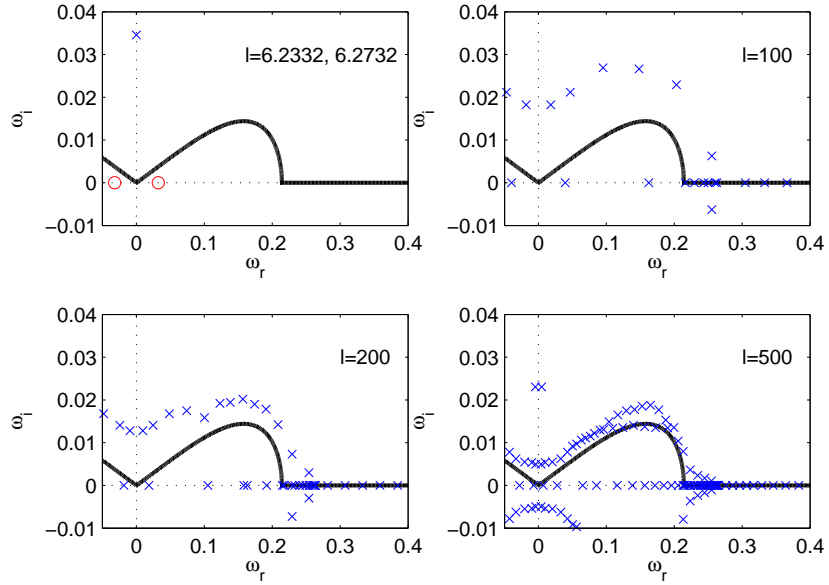
#### 4.2.2 Effect of damping on marginal stability of the clamped-free pipe

The global stability of the system is now characterized by plotting in the  $(\beta, l)$  plane the marginal stability curve on Fig. 3a for  $c = 0$  (no damping). This curve corresponds to the line in the  $(\beta, l)$  plane where the maximum growth rate  $\max_n[\text{Im}(\omega_n)] = 0$ . On the same figure, the local stability criterion  $\beta = 1$  is plotted. It appears then that the long system limit for global instability is the local stability criterion. On Fig. 3b, different values of the dimensionless damping  $c$  from 0 to 1000 are considered. The resulting marginal stability curve move continuously from the undamped limit to an horizontal limit. For  $\beta \in [0, 0.2]$ , the damping appears to have a stabilizing effect while it has a destabilizing effect for  $\beta > 0.2$ . Hence also for the finite length clamped-free pipe, damping can have a destabilizing effect. While in absence of damping, the instability criterion of the finite length tends to the local one when  $l$  is increased, no such limit can be observed in the damped case because the damped medium is locally unstable  $\forall \beta$ . However, the horizontal limit observed at high values of the damping cannot be predicted by a local criterion.

#### 4.2.3 Kulikovskii's criterion

We have observed in section 4.2.2 that the long system limit of the marginal stability curve in the undamped case is the local stability criterion. In the case of the Ginzburg-Landau equation, which is a simplified amplitude equation describing fluid-mechanics systems such as jets, vortices or shear layers, the long system limit for global instability criterion was found to be that of transition from local convective instability to absolute instability [37, 11]. Convective and absolute instabilities distinguish the long time behavior the temporally growing wave packet generated by an impulse forcing on an unstable medium. In the

### Clamped-clamped pipe $\beta = 0.95$



### Clamped-free pipe $\beta = 0.95$

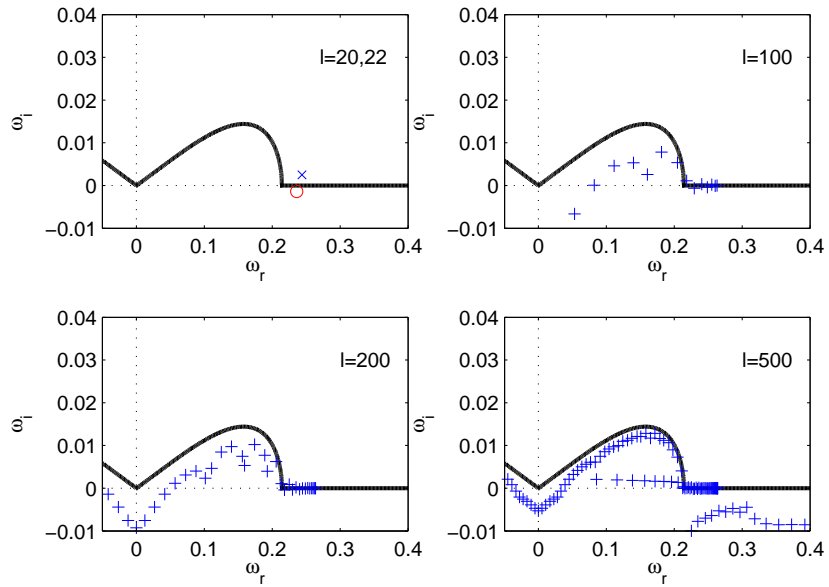


Figure 4: Eigenfrequencies of the clamped-clamped and clamped-free pipe at  $\beta = 0.95$  and for different values of the length  $l$ , compared to the kulikovskii criterion. In the upper-left plot of each case, the circles and crosses represent the locii of the eigenvalues just below and just above the instability threshold respectively. These plots illustrate the fact that although the apparition of instability is different between these two sets of boundary conditions, all the eigenfrequencies approach a common limit when the length of the system is increased to infinity.

case of convective instability, the growing wave packet is advected by the stream, while in the case of absolute instability, the wave packet grows in place. For the fluid-conveying pipe, the transition between these two kind of local instabilities occurs at  $\beta = 8/9$  [21].

Hence the long system limit is predicted by a local criterion, which is not unique. A criterion introduced by Kulikovskii in 1966 in the context of electron beam instability and cited in the book by Lifshitz and Pitaevskii [26] permits to determine which local criterion should prevail. Kulikovskii showed that as the length of the system tends to infinity, the eigenvalues tend to a continuous line in the complex frequency plane such that the most spatially amplified (or least evanescent) downstream propagating wave is exactly balanced by the least spatially evanescent (or most amplified) upstream propagating wave, which is formally written as:

$$\text{Im}(k^+ - k^-) = 0, \quad (26)$$

where  $k^+$  is the downstream wavenumber that has the minimum imaginary part, and  $k^-$  is the upstream wavenumber that has the maximum imaginary part. It can be shown in the fluid mechanics media mentioned above that in case of convective instability, no frequency of positive imaginary part satisfies this criterion. Conversely, it is possible to satisfy this criterion with unstable frequencies in the fluid conveying pipe case when convectively unstable. Consequently, in the long system limit, the convectively unstable pipe is unstable while it is not the case for the Ginzburg-Landau equation. To illustrate this phenomenon, the Kulikovskii criterion is plotted on Fig. 4 in the complex plane of frequencies and compared to the locii of eigenfrequencies when the length of the system is increased to large values. The value of  $\beta = 0.95$  is chosen so that the medium is convectively unstable. Two different sets of boundary conditions are presented. It appears that although the occurrence of bifurcations are different in both systems, the eigenfrequency maps converge to the same limit when  $l \rightarrow \infty$ .

#### 4.2.4 Lengthscale criterion

We have discussed in the previous section the long system limit. We now address the opposite case of short systems. On figure 3a, for the values of the parameters comprised between the local and global stability curves, and below the dashed lines on figure 3b the system is globally stable although locally unstable. In this situation, the confinement induced by considering a short system has for consequence to prevent unstable waves to play a role in the dynamics. This confinement effect can be quantified and can give an approximate criterion of stability. Let us state that an unstable wave can give rise to an unstable mode of the finite system only if its wavelength is smaller than the length of the system. The smallest unstable wavelengths are,

$$\lambda = \frac{2\pi}{\sqrt{1-\beta}}, \quad \lambda_d = 2\pi, \quad (27)$$

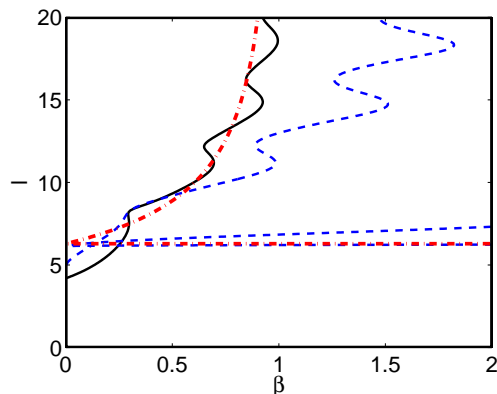


Figure 5: Global stability curves of the pipe conveying fluid in the  $(\beta, l)$  plane for increasing values of the viscous damping (plain and dashed lines), compared with the length criteria defined in equation (27) (dash-dotted lines).

in the undamped and damped cases respectively. Plotted against the marginal stability curves on Fig. 5, these criteria show a good agreement. The marginal stability curve goes continuously from the length criterion without damping to that with damping.

## 5 Application to energy harvesting

The possibility to take profit of the energy transfer between a flow and a structure through the flutter phenomenon has recently received a significant amount of attention. Various harvesting systems have been considered theoretically or experimentally, such as the simple Kelvin-Voigt type dampers [33], electromagnetic coupling [35] or piezoelectric coupling [15, 1, 28]. In this section, we summarize a study of a clamped-free plate equipped with a continuous distribution of piezoelectric patches [15]. The piezoelectric effect couples deformation in the plate to the electric field and electrical energy may then be harvested at the outlets of a piezoelectric patch. Although more sophisticated circuits can be considered [24], in the model presented here, the harvested energy is that dissipated in a shunting resistance. The dimensionless model presented here takes the form of two coupled wave equations for the the vertical displacement of the plate  $y$  and the electrical charge displacement per unit length  $q$  :

$$\frac{1}{V^2} (1 + \alpha^2) \frac{\partial^4 y}{\partial x^4} + \frac{\partial^2 y}{\partial t^2} - \frac{\alpha}{V} \frac{\partial^2 q}{\partial x^2} = -[p], \quad (28)$$

$$\gamma \frac{\partial q}{\partial t} + q - \frac{\alpha}{V} \frac{\partial^2 w}{\partial x^2} = 0. \quad (29)$$

In (28), the two first terms are the rigidity and inertia terms of the linear Euler-Bernoulli beam model, the third term quantifies the momentum exerted on the

plate consecutively to the electric field in the piezoelectric patches and the right-hand term is the pressure jump between both sides of the plate. The latter can be written as a linear function of the small amplitude displacement  $y$  and its effective expression may take different forms depending on the approximations and geometries of the system. For instance, if the typical length of deformation is large compared to the width of the plate, the pressure jump has the same three fluid terms as in the fluid conveying pipe equation (8) [25]. In the opposite case of an infinite span plate, one gets the same three terms, scaled by  $1/k$  where  $k$  is the wavenumber [12]. In equation (29), the first two terms stand for the Ohm's law, while the third term expresses the inverse piezoelectric coupling: a deformation in the piezoelectric material leads to an electrical charge displacement. The parameters of the problem are  $V$ , the nondimensional flow velocity,  $\alpha$ , the piezoelectric coupling coefficient, and  $\gamma$  is the ratio between the fluid-solid and electrical characteristic timescales.

The uncoupled medium ( $\alpha = 0$ ) bears temporally unstable waves, as well as neutral waves, some of them being negative energy waves. An analysis similar to that performed in section 4.1 shows that the temporal growth rate of neutral waves is perturbed by the following amount when piezoelectric coupling is added:

$$\delta\sigma \simeq \frac{\omega\alpha^2\gamma k^4}{V^2(1 + \omega^2\gamma^2)\frac{\partial D}{\partial\omega}} \cdot \cdot \quad (30)$$

This expression shows that the perturbation of the growth rate has the opposite sign of the wave energy and scales as  $\alpha^2$ . Piezoelectric coupling hence destabilizes negative energy waves. Moreover,  $\delta\sigma$  presents a maximum when  $\gamma = 1/\omega$ , that is when the time scale of the  $RC$  circuit is the same as that of the wave.

In the linear analysis, the conversion efficiency of the system can be defined for an unstable wave, as the ratio between the power dissipated in the resistances during one period, and the mean of the energy present in the system over this same period.

It is found in [15] that the maximum efficiency is always maximized for a negative energy wave destabilized by piezoelectric coupling, when  $\gamma \sim 1/\omega$ . In other words, energy harvesting may destabilize negative energy waves, and conversion efficiency is maximized with these waves.

The finite length system may also be analyzed and similar results as in the case of the fluid-conveying pipe are found. The system can indeed be destabilized or stabilized by piezoelectric coupling. An analysis of the efficiency of the conversion shows that the maximum efficiency exists in the domain of parameters where destabilization by piezoelectric coupling occurs. It happens for long systems, which originates from the same confinement effect discussed in the previous section.

## 6 Conclusion

The counter-intuitive effect of damping on the stability fluid-conveying pipe has been analysed both in terms of waves propagating in the infinite medium (local approach) and in terms of modes in the finite length system (global approach). The fluid-conveying pipe is a model problem for many fluid-elastic system where a compliant structure interacts with a flow, such as flags, plates, shells, walls or wings.

It was shown that the Coriolis force has a stabilizing effect on the infinite medium and that damping cancels this effect. The destabilizing effect of damping was shown to be due to the creation of negative energy waves by the Coriolis term. The finite length system can be stabilized or destabilized by damping. A lengthscale analysis has shown that destabilization by damping may be due to the destabilization of negative energy waves. In references [14, 13], additional rigidity forces are considered on the pipe, such as elastic foundation or tension. A more rich picture of stability properties is then evidenced.

Extension to energy harvesting systems has been briefly addressed. It was shown that energy harvesting has a similar destabilizing effect on such fluid-elastic systems and that negative energy waves maximize energy conversion efficiency.

## References

- [1] D. T. Akcabay and Y. L. Young. Hydroelastic response and energy harvesting potential of flexible piezoelectric beams in viscous flow. *Physics of Fluids*, 24(5):054106, 2012.
- [2] J. Antunes, F. Axisa, and T. Grunewald. Dynamics of rotors immersed in eccentric annular flow. Part 1: Theory. *Journal of Fluids and Structures*, 10(8):893–918, 1996.
- [3] M. Beck. Die Knicklast des einseitig eingespannten tangential gedruckten stabes. *Z. Angew. Math. Phys.*, 3:225–229, 1952.
- [4] G. Bekefi and Howard H. C. Chang. Radiation Processes in Plasmas. *Physics Today*, 22(1):103–107, 1969.
- [5] D. Bigoni. *Nonlinear Solid Mechanics, Bifurcation Theory and Material Instability*. 2012.
- [6] D. Bigoni and G. Noselli. Experimental evidence of flutter and divergence instabilities induced by dry friction. *Journal of the Mechanics and Physics of Solids*, 59:2208–2226, 2011.
- [7] R.D. Blevins. *Flow-induced vibration*. 1990.
- [8] O. Bottema. On the stability of the equilibrium of a linear mechanical system. *Z. Angew. Math. Phys.*, 6:97–104, 1955.

- [9] R. J. Briggs. *Electron-Stream Interaction with Plasmas*. The MIT Press, 1964.
- [10] R. A. Cairns. The role of negative energy waves in some instabilities of parallel flows. *Journal of Fluid Mechanics*, 92:1–14, 1979.
- [11] C. Cossu and J. M. Chomaz. Global measures of local convective instabilities. *Physical Review Letters*, 78(23):4387–4390, JUN 9 1997.
- [12] D. Crighton and J. E. Oswell. Fluid loading with mean flow. I. Response of an elastic plate to localized excitation. *Philosophical Transactions of the Royal Society of London A*, 335:557–592, 1991.
- [13] O. Doaré. Dissipation effect on local and global stability of fluid-conveying pipes. *Journal of Sound and Vibration*, 329(1):72–83, 2010.
- [14] O. Doaré and E. de Langre. Local and global stability of fluid-conveying pipes on elastic foundations. *Journal of FLuids and Structures*, 16(1):1–14, 2002.
- [15] O. Doaré and S. Michelin. Piezoelectric coupling in energy-harvesting fluttering flexible plates: linear stability analysis and conversion efficiency. *Journal of Fluids and Structures*, 27(8):1357–1375, 2011.
- [16] R. W. Gregory and M. P. Paidoussis. Unstable oscillation of tubular cantilevers conveying fluids. I. Theory. *Proceedings of the Royal Society of London, A* 293:512–527, 1966.
- [17] T. Grunewald, F. Axisa, G. Bennett, and J. Antunes. Dynamics of rotors immersed in eccentric annular flow. Part 2: Experiments. *Journal of Fluids and Structures*, 10(8):919–944, 1996.
- [18] C. Q. Guo and M. P. Paidoussis. Stability of Rectangular Plates With Free Side-Edges in Two-Dimensional Inviscid Channel Flow. *Journal of Applied Mechanics*, 67(1):171–176, 2000.
- [19] O. N. Kirillov. Gyroscopic stabilization in the presence of nonconservative forces. *Doklady Mathematics*, 76(2):780–785, 2007.
- [20] O. N. Kirillov and F. Verhulst. Paradoxes of dissipation-induced destabilization or who opened Whitney’s umbrella? *Z. Angew. Math. Mech.*, 90(6):462–488, 2010.
- [21] A. G. Kulikovskii and I. S. Shikina. On the bending oscillations of a long tube filled with moving fluid. *Izv. Akad. Nauk. ArmSSR, Mekhanika*, 41(1):31–39, 1988.
- [22] M. T. Landahl. On the stability of a laminar incompressible boundary layer over a flexible surface. *Journal of FLuid Mechanics*, 13(4):609–632, 1962.



- [23] B. H. K. Lee, L. Gong, and Y. S. Wong. Analysis and computation of nonlinear dynamic response of a two degree of freedom system and its application in aeroelasticity. *Journal of Fluids and Structures*, 11(3):225–246, 1997.
- [24] E. Lefeuvre, A. Badel, C. Richard, L. Petit, and D. Guyomar. A comparison between several vibration-powered piezoelectric generators for standalone systems. *Sensors and Actuators A: Physical*, 126(2):405–416, 2006.
- [25] C. Lemaitre, P. Hémon, and E. de Langre. Instability of a long ribbon hanging in axial air flow. *Journal of Fluids and Structures*, 20(7):913–925, 2005.
- [26] E. M. Lifshitz and L.P. Pitaevskii. *Physical Kinetics (Course of Theoretical Physics)*, volume 10. Butterworth-Heinemann, 1981.
- [27] I. Lottati and A. Kornecki. The effect of an elastic foundation and of dissipative forces on the stability of fluid-conveying pipes. *Journal of Sound and Vibration*, 2(109):327–338, 1986.
- [28] S. Michelin and O. Doaré. Energy harvesting efficiency of piezoelectric flags in axial flows. *Journal of Fluid Mechanics*, 714:489-504, 2013.
- [29] M. P. Païdoussis. *Fluid-Structure Interactions : Slender Structures and Axial Flow*, volume 2. Academic Press, 1998.
- [30] M. P. Païdoussis. The canonical problem of the fluid-conveying pipe and radiation of the knowledge gained to other dynamics problems across Applied Mechanics. *Journal of Sound and Vibration*, 310(3):462–492, 2008.
- [31] W. Roth. Instabilität durchströmter Rohre. *Ingenieur-Archiv*, 33:236–263, 1964.
- [32] M. Ruijgrock, A. Tondl, and F. Verhulst. Resonance in a rigid rotor with elastic support. *Z. Angew. Math. Mech.*, 73:255–263, 1993.
- [33] K. Singh, S. Michelin, and E. de Langre. Energy harvesting from fluid-elastic instabilities of a cylinder. *Journal of Fluids and Structures*, in press, 2012.
- [34] Y. Sugiyama and M. A. Langthjem. Physical mechanism of the destabilizing effect of damping in continuous non-conservative dissipative systems. *International Journal of Non-Linear Mechanics*, 42(1):132–145, 2007. Non-linear Dynamic Stability of Nonconservative Dissipative Systems.
- [35] L. Tang and M. P. Païdoussis. The coupled dynamics of two cantilevered flexible plates in axial flow. *Journal of Sound and Vibration*, 323(3-5):790–801, 2009.
- [36] W. Thomson and P. G. Tait. *Treatise on Natural Philosophy*. Cambridge University Press, 1879.

- [37] S. M. Tobias, M. R. E. Proctor, and E. Knobloch. Convective and absolute instabilities of fluid flows in finite geometry. *Physica D: Nonlinear Phenomena*, 113(1):43–72, 1998.
- [38] M. von Laue. The Propagation of Radiation in Dispersive and Absorbing Media. *Ann. Physik*, 1905.
- [39] H. Whitney. The general type of singularity of a set of  $2n - 1$  smooth functions of  $n$  variables. *Duke Math. J.*, 10:161–172, 1943.
- [40] H. Ziegler. Die stabilitätskriterien der elastomechanik. *Ing.-Arch*, 20:49–56, 1952.